**Supporting Information:**

Erwin Reisner, Vladimir B. Arion,* Anna Eichinger, Norbert Kandler, Gerald Giester, Armando J. L. Pombeiro,* and Bernhard K. Keppler*

**Tuning of Redox Properties for the Design of Ruthenium Anticancer Drugs: Part 2. Syntheses, Crystal Structures and Electrochemistry of Potentially Antitumor $[Ru^{III/II}Cl_{6-n}(azole)_n]^z$ (n = 3,4,6) Complexes**



**Crystal structures.** Complex **B1**. The dihedral angles of mutually *trans* butylimidazole ligands are –30.6 and –9.9° in **B1a** and **B1b**, correspondingly. The butylimidazol ligands coordinated to ruthenium via N10 and N19 in **B1a** are tilted relative to the mean plane through Ru1N10N19Cl1Cl3, the corresponding angles being at 36.7 and 6.3°. In **B1b** the dihedral angles between imidazole rings bonded to ruthenium via N37 and N46, and the mean plane through Ru2N37N46Cl4Cl6 are at 45.2 and 35.6°, respectively. The imidazole rings ligated to ruthenium via N1 and N28 nearly bisect the angles Cl3Ru1N10 and Cl6Ru2N46, the torsion angles $\Theta_{C2N1Ru1Cl3}$ and $\Theta_{C29N28Ru2Cl6}$ being at –38.60(15) and 33.90(15)°, correspondingly.

Complex **B4**. The bond angles at the ruthenium center have almost idealized values; the largest deviations from 90 and 180° were found for Cl3–Ru–Cl2 at 92.67(3)° and N4–Ru–N10 at 176.94(7)°. The triazole ligands coordinated *via* N4 and N10 are tilted relative to the mean plane through RuN4N10Cl1Cl3, the corresponding angles being at 48.7 and 14.5°, while the triazole ligand ligated *via* N16 nearly bisects the angle Cl1–Ru–N4, the torsion angle $\Theta_{Cl1RuN16C15}$ being at 37.87(19)°.

Complex **B5**. The 4-methylpyrazole ligands linked to the Ru atom *via* N1 and N7 are nearly coplanar to the mean planes through RuCl1Cl2Cl3N1 and RuCl2N1N7N13, correspondingly. The torsion angles

$\Theta_{N1RuN7C11}$ and $\Theta_{Cl3RuN1N2}$ are at –4.25(18) and 2.31(15)°, respectively. The third azole ring ligated to Ru atom *via* N13 is tilted to the RuCl2N7N1N13 mean plane by ~ 26°.

Complex **B6**·$H_2O$. The triazole ligand ligated *via* N2 bisects the angle Cl1–Ru–N3, the torsion angle $\Theta_{Cl1RuN2C3}$ being at –45.44(15)°. The other two torsion angles $\Theta_{Cl3RuN7N6}$ and $\Theta_{Cl3RuN12C13}$ indicating the position of triazole ligands coordinated *via* N7 and N12 are at 48.38(12) and –48.52(15)°, respectively.

Complex **B7**. The pyrazole ligands *trans* to each other are almost coplanar in both cases, the corresponding dihedral angle being at 1.7 (**B7a**) and 3.8° (**B7b**). Their position in respect to the Ru1N6N11Cl1Cl3 and Ru2N21N26Cl4Cl6 can be defined by torsion angles $\Theta_{N12N11Ru1Cl3}$ at –29.1(2) and $\Theta_{N7N6Ru1Cl3}$ at 30.14(18)° in molecule **B7a** and $\Theta_{Cl6Ru2N21C25}$ at 156.2(2) and $\Theta_{Cl6Ru2N26C30}$ at –154.6(2)° in **B7b**. The positions of the pyrazole rings bonded to ruthenium through N1 and N16 in respect to Ru1Cl1Cl2Cl3N1 and Ru2Cl4Cl5Cl6N16 are defined by the torsion angles $\Theta_{N2N1Ru1Cl3}$ at –18.63(18)° and $\Theta_{N17N16Ru2Cl6}$ at 40.75(18)°.

Complex **C2**. The orientation of the imidazole rings with respect to the Ru–Cl1 vector is almost staggered, the $\Theta_{C3N1RuCl1}$ and $\Theta_{C6N3RuCl1}$ torsion angles being at 45.63(11) and 50.48(11)°.

Complex **C3**·$CH_3OH$·$(C_2H_5)_2O$. The orientation of benzimidazole ligands in respect to Ru–Cl1 and Ru–Cl2 vectors is very similar, tending to minimize steric crowding between them and is determined by torsion angles $\Theta_{C1N1RuCl1}$ at –41.35(13), $\Theta_{C8N3RuCl1}$ at –44.66(12), $\Theta_{C21N5RuCl2}$ at –45.79(14) and $\Theta_{C28N7RuCl2}$ at –45.41(14)°.

Complex **C6a**·$2H_2O$. The orientation of the Htrz planes with respect to the Ru–Cl vector is almost staggered, the $\Theta_{C3N2RuCl}$ and $\Theta_{N6N7RuCl}$ torsion angles being at 31.8(3) and 30.3(3)°, respectively.

Complex **C7**. The *trans*-coordinated pyrazole ligands are parallel to each other. The dihedral angle between them is small and does not exceed 1°. The N–N bonds in *trans*-coordinated ligands are also *trans* to each other. The orientation of pyrazole ligands in respect to Ru–Cl1 and Ru–Cl2 vectors is described by the torsion angles $\Theta_{C5N1Ru1Cl1}$ at –17.61(16), $\Theta_{N7N6Ru1Cl1}$ at 24.20(13), $\Theta_{N12N11Ru2Cl2}$ at –33.33(14) and $\Theta_{N17–N16–Ru2–Cl2}$ at 21.67(14)°. Both the coordinated chloro ligands and the chloride counter anions are involved in hydrogen bonding interactions.

**Table S1.** Selected Bond Distances (Å) and Angles (°) in Two Independent Molecules of **B1**

| Atom1−Atom2 | **B1a** | Atom1−Atom2 | **B1b** |
|---|---|---|---|
| Ru1−N1 | 2.0623(15) | Ru2−N28 | 2.0670(15) |
| Ru1−N10 | 2.0768(14) | Ru2−N37 | 2.0763(15) |
| Ru1−N19 | 2.0886(14) | Ru2−N46 | 2.0744(15) |
| Ru1−Cl1 | 2.3602(6) | Ru2−Cl4 | 2.3597(6) |
| Ru1−Cl2 | 2.3696(6) | Ru2−Cl5 | 2.3800(6) |
| Ru1−Cl3 | 2.3603(6) | Ru2−Cl6 | 2.3522(6) |
| Atom1-Atom2-Atom3 | | Atom1-Atom2-Atom3 | |
| N10–Ru1–N19 | 176.88(6) | N37–Ru2–N46 | 178.02(6) |
| N1–Ru1–Cl2 | 178.55(4) | N28–Ru2–Cl5 | 177.94(4) |
| Cl1–Ru1–Cl3 | 178.343(15) | Cl4–Ru2–Cl6 | 178.389(16) |

**Table S2.** Selected Interatomic Bond Distances (Å) and Angles (°) in **B4**

| Atom1−Atom2 | Å | Atom1−Atom2 | Å |
|---|---|---|---|
| Ru1−N4 | 2.0691(18) | Ru1−Cl1 | 2.3627(7) |
| Ru1−N10 | 2.0864(18) | Ru1−Cl2 | 2.3541(8) |
| Ru1−N16 | 2.0748(19) | Ru1−Cl3 | 2.3395(6) |
| Atom1-Atom2-Atom3 | deg | Atom1-Atom2-Atom3 | deg |
| N4–Ru1–N10 | 176.94(7) | N16–Ru1–Cl2 | 177.30(5) |
| Cl1–Ru1–Cl3 | 177.37(2) | | |

**Table S3.** Selected Bond Distances (Å) and Angles (°) in **B5**

| Atom1−Atom2 | Å | Atom1−Atom2 | Å |
|---|---|---|---|
| Ru1−N1 | 2.0793(17) | Ru1−Cl1 | 2.3468(6) |
| Ru1−N7 | 2.0576(16) | Ru1−Cl2 | 2.3912(6) |
| Ru1−N13 | 2.0504(16) | Ru1−Cl3 | 2.3413(6) |
| Atom1-Atom2-Atom3 | deg | Atom1-Atom2-Atom3 | deg |
| N7−Ru1−N13 | 178.50(7) | N1−Ru1−Cl2 | 178.66(5) |
| Cl1−Ru1−Cl3 | 178.654(19) | | |

**Table S4.** Selected Bond Distances (Å) and Angles (°) in **B6**·$H_2O$

| Atom1−Atom2 | Å | Atom1−Atom2 | Å |
|---|---|---|---|
| Ru1−N2 | 2.0764(15) | Ru1−Cl1 | 2.3434(7) |
| Ru1−N7 | 2.0734(16) | Ru1−Cl2 | 2.3469(6) |
| Ru1−N12 | 2.0667(16) | Ru1−Cl3 | 2.3427(8) |
| Atom1-Atom2-Atom3 | deg | Atom1-Atom2-Atom3 | deg |
| N7−Ru1−N12 | 178.66(6) | N2−Ru1−Cl2 | 179.51(4) |
| Cl1−Ru1−Cl3 | 178.539(16) | | |

**Table S5.** Selected Bond Distances (Å) and Angles (°) in Two Independent Molecules in **B7**

| Atom1−Atom2 | **B7a** | Atom1−Atom2 | **B7b** |
|---|---|---|---|
| Ru1−N1 | 2.073(2) | Ru2−N16 | 2.0630(19) |
| Ru1−N6 | 2.0527(19) | Ru2−N21 | 2.0665(19) |
| Ru1−N11 | 2.0600(19) | Ru2−N26 | 2.0641(19) |
| Ru1−Cl1 | 2.3584(8) | Ru2−Cl4 | 2.3536(8) |
| Ru1−Cl2 | 2.3552(9) | Ru2−Cl5 | 2.3539(8) |
| Ru1−Cl3 | 2.3777(8) | Ru2−Cl6 | 2.3820(8) |
| Atom1-Atom2-Atom3 | | Atom1-Atom2-Atom3 | |
| N6–Ru1–N11 | 177.54(8) | N21–Ru2–N26 | 179.28(7) |
| N1–Ru1–Cl2 | 178.37(5) | N16–Ru2–Cl5 | 179.06(5) |
| Cl1–Ru1–Cl3 | 179.41(2) | Cl4–Ru2–Cl6 | 177.61(2) |

**Table S6.** Selected Bond Distances (Å) and Angles (°) in **C2**

| Atom1−Atom2 | Å | Atom1−Atom2 | Å |
|---|---|---|---|
| Ru1−N1 | 2.0687(12) | Ru1−N3 | 2.0682(12) |
| Ru1−Cl1 | 2.3379(6) | Ru1−Cl2 | 2.3458(6) |
| Atom1-Atom2-Atom3 | deg | Atom1-Atom2-Atom3 | deg |
| N3–Ru1–N1 | 90.19(5) | N3–Ru1–Cl1 | 90.43(3) |
| N1–Ru1–Cl1 | 90.34(3) | N3–Ru1–Cl2 | 89.57(3) |
| N1–Ru1–Cl2 | 89.66(3) | Cl1–Ru1–Cl2 | 180.0 |

**Table S7.** Selected Bond Distances (Å) and Angles (°) in **C3**·$CH_3OH$·$(C_2H_5)_2O$

| Atom1–Atom2 | Å | Atom1–Atom2 | Å |
|---|---|---|---|
| Ru1–N1 | 2.0862(15) | Ru1–N7 | 2.0792(14) |
| Ru1–N3 | 2.0697(14) | Ru1–Cl1 | 2.3570(8) |
| Ru1–N5 | 2.0732(15) | Ru1–Cl2 | 2.3232(8) |
| Atom1-Atom2-Atom3 | deg | Atom1-Atom2-Atom3 | deg |
| N1–Ru1–N5 | 177.14(5) | N3–Ru1–N7 | 178.09(5) |
| Cl1–Ru1–Cl2 | 178.601(15) | | |

**Table S8.** Selected Bond Distances (Å) and Angles (°) in **C6**·$2H_2O$

| Atom1–Atom2 | Å | Atom1–Atom2 | Å |
|---|---|---|---|
| Ru1–N2 | 2.073(3) | Ru1–N7 | 2.074(3) |
| Ru1–Cl1 | 2.3289(10) | | |
| Atom1-Atom2-Atom3 | deg | Atom1-Atom2-Atom3 | deg |
| N2–Ru1–N7 | 86.84(12) | N2–Ru1–Cl1 | 89.58(9) |
| N7–Ru1–Cl1 | 91.07(9) | | |

**Table S9.** Selected Bond Distances (Å) and Angles (°) in **C7**

| Atom1−Atom2 | Å | Atom1−Atom2 | Å |
|---|---|---|---|
| Ru1−N1 | 2.0557(15) | Ru2−N11 | 2.0624(15) |
| Ru1−N6 | 2.0571(15) | Ru2−N16 | 2.0659(18) |
| Ru1−Cl1 | 2.3767(9) | Ru2−Cl2 | 2.3565(7) |
| Atom1-Atom2-Atom3 | deg | Atom1-Atom2-Atom3 | deg |
| N1−Ru1−N6 | 89.14(6) | N11−Ru2−N16 | 93.03(6) |
| N1−Ru1−Cl1 | 90.86(5) | N11−Ru2−Cl2 | 91.09(5) |
| N6−Ru1−Cl1 | 89.13(5) | N16−Ru2−Cl2 | 89.34(5) |

**Table S10.** UV-vis Absorption Bands [Wavelength and Molar Absorptivity (in Brackets)] for Complexes **B** and **C** in Methanol at 298K used for the establishment of equations (3) and (4). The metal-centered $Ru^{III}/Ru^{II}$ redox potential increases with the increase of the absorption wavelengths $\lambda$ (Fig. S7)

| Complex | $\lambda_{max}$ (nm) / $\varepsilon$ ($mM^{-1}cm^{-1}$) | Complex | $\lambda_{max}$ (nm) / $\varepsilon$ ($mM^{-1}cm^{-1}$) |
|---|---|---|---|
| **B1** | 347 (3.29) | **C2** | 346 (2.71) |
| **B3** | 358 (3.12) | **C3** | 363 (2.67) |
| **B4** | 371 (3.55) | **C6** | 400 (2.77) |
| **B5** | 369 (3.08) | **C7** | 401 (3.71)[a] |
| **B6**·$H_2O$ | 376 (3.35) | **C8** | 452 (2.69) |
| **B7** | 376 (3.18) | | |
| **B8** | 381 (3.71) | | |

[a] overlapped band

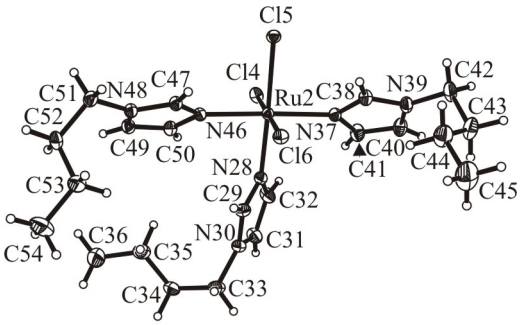


**Fig. S1.** ORTEP view of the second independent molecule of $[Ru^{III}Cl_3(buim)_3]$ (**B1b**), showing the atom-numbering scheme. Thermal displacement ellipsoids are drawn at the 50% probability level.

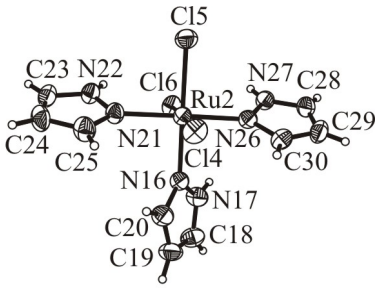


**Fig. S2.** ORTEP view of the second independent molecule of $[Ru^{III}Cl_3(Hpz)_3]$ (**B7b**), showing the atom-numbering scheme. Thermal displacement ellipsoids are drawn at the 50% probability level.

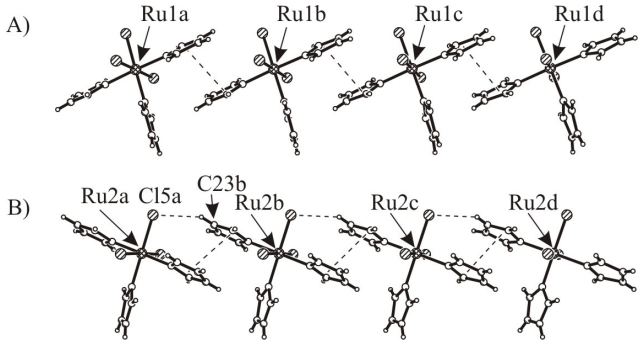


**Fig. S3.** Infinite chains in **B7** formed by the two independent molecules **B7a** (A) and **B7b** (B), which are stabilized by stacking $\pi$–$\pi$ interactions between *trans*-coordinated pyrazole ligands of adjacent molecules and *inter*molecular hydrogen bonding.

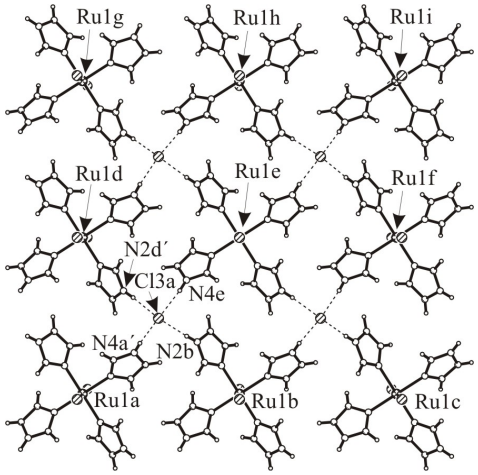


**Fig. S4.** N–H···Cl hydrogen bonding interactions of $[Ru^{III}Cl_2(Him)_4]Cl$ (**C2**) parallel to ac cell planes.

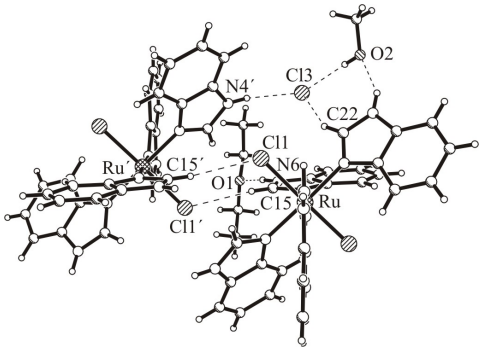


**Fig. S5.** A part of the crystal structure of **C3**·$CH_3OH$·$(C_2H_5)_2O$ showing the formation of multiple hydrogen bonds between the complex cations, counter anion and solvent molecules.

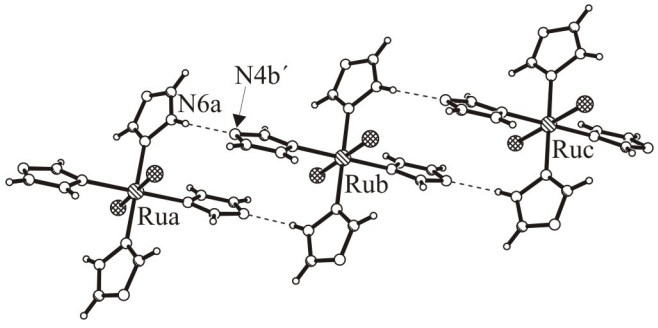


**Fig. S6.** Parallel chains in the structure of **C6a**·$2H_2O$, which are stabilized by strong *intra*chain hydrogen bonding interactions between $[Ru^{III}Cl_2(Htrz)_4]^+$.

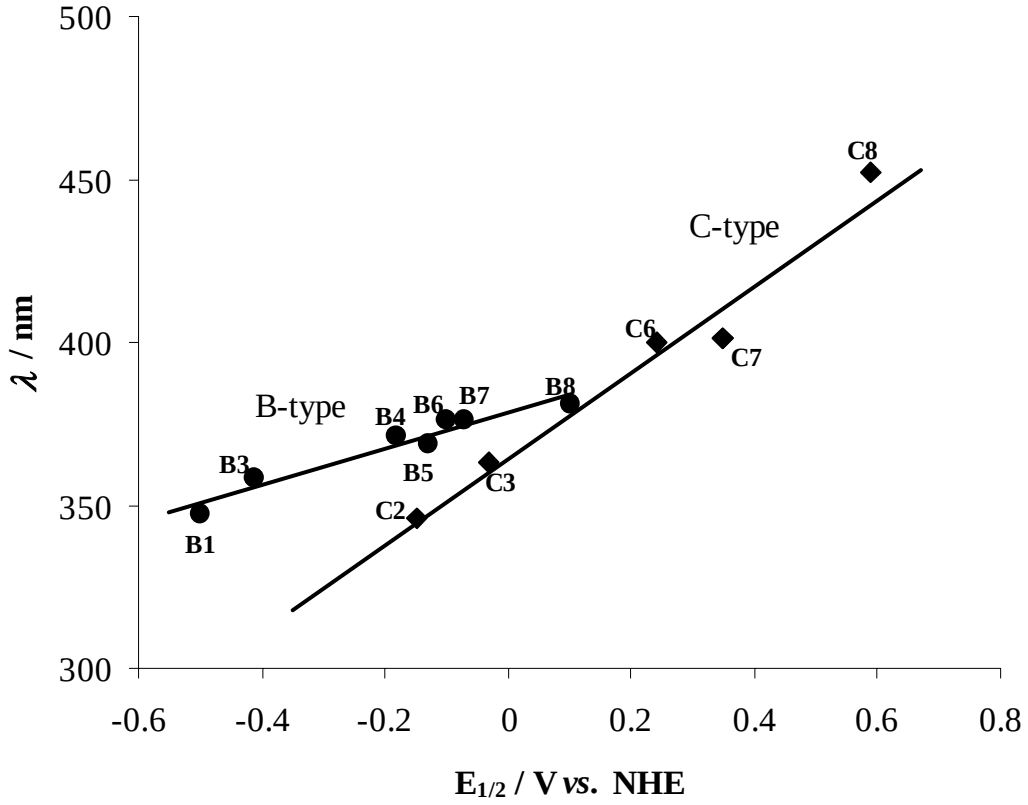


**Fig. S7.** Plot of the UV-vis absorption bands against $E_{½}$ ($Ru^{III}/Ru^{II}$) for complexes **B** (●) and **C** (♦). The electrochemical data is shown in Table 3 and the optical data in Table S10: $\lambda$ (nm) = 55.9 $E_{½}$ (V) + 378.6 (r = 0.97) (**B**) and $\lambda$ (nm) = 136.1 $E_{½}$ (V) + 365.2 (r = 0.99) (**C**).

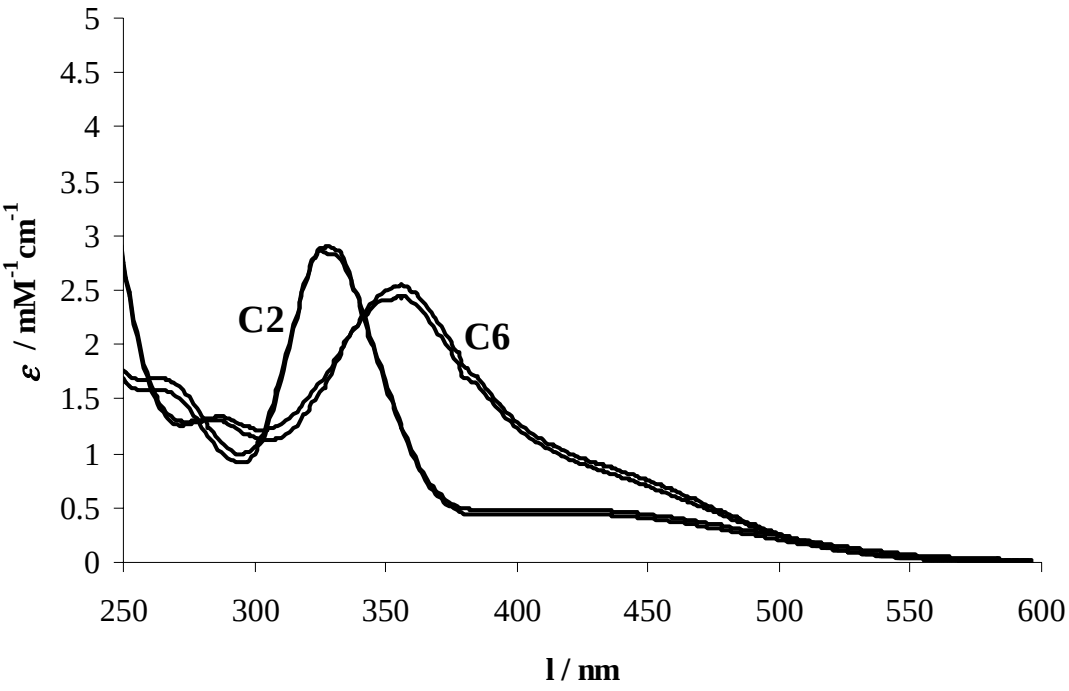


**Fig. S8.** The electronic absorption spectra of **C2** [measured directly after dissolution (upper line) and after 24 h (lower line)] and **C6** [measured directly after dissolution (upper line) and after 3 h (lower line)] in 0.2 M phosphate buffer at pH 7.0 at room temperature.